

Long-range interactions & parallel scalability in molecular simulations

Michael Patra ^a

^a *Physical Chemistry I, Lund University, Sweden*

Marja T. Hyvönen ^b

^b *Wihuri Research Institute, Helsinki, Finland; Laboratory of Physics and Helsinki Institute of Physics, Helsinki University of Technology, Finland*

Emma Falck ^c

^c *Beckman Institute for Advanced Science and Technology, University of Illinois at Urbana-Champaign, Urbana (IL), U.S.A.*

Mohsen Sabouri-Ghomi ^d

^d *Department of Biology, Virginia Polytechnic Institute & State University Blacksburg (VA), U.S.A.; Department of Cell Biology, The Scripps Research Institute, La Jolla (CA), U.S.A.*

Ilpo Vattulainen ^e

^e *Institute of Physics, Tampere University of Technology, Tampere, Finland; Laboratory of Physics and Helsinki Institute of Physics, Helsinki University of Technology, Finland; University of Southern Denmark, Odense, Denmark*

Mikko Karttunen ^f

^f *Department of Applied Mathematics, the University of Western Ontario, London, Ontario, Canada.*

Abstract

Typical biomolecular systems such as cellular membranes, DNA, and protein complexes are highly charged. Thus, efficient and accurate treatment of electrostatic interactions is of great importance in computational modelling of such systems. We have employed the GROMACS simulation package to perform extensive benchmarking of different commonly used electrostatic schemes on a range of computer architectures (Pentium-4, IBM Power 4, and Apple/IBM G5) for single processor

and parallel performance up to 8 nodes – we have also tested the scalability on four different networks, namely Infiniband, GigaBit Ethernet, Fast Ethernet, and nearly uniform memory architecture, i.e., communication between CPUs is possible by directly reading from or writing to other CPUs’ local memory. It turns out that the particle-mesh Ewald method (PME) performs surprisingly well and offers competitive performance unless parallel runs on PC hardware with older network infrastructure are needed. Lipid bilayers of sizes 128, 512 and 2048 lipid molecules were used as the test systems representing typical cases encountered in biomolecular simulations. Our results enable an accurate prediction of computational speed on most current computing systems, both for serial and parallel runs. These results should be helpful in, for example, choosing the most suitable configuration for a small departmental computer cluster.

Key words: molecular simulations, parallel computing, electrostatics, lipid membranes, GROMACS

1 Introduction

During the last few decades, molecular modelling has emerged as an indispensable tool in studies of soft-matter and biological systems providing information not accessible by current experimental techniques [1,2,3,4,5,6]. One of the challenges in modelling biomolecular systems is the fact that their properties are largely dictated by electrostatics. At the same time, biosystems are large – especially when compared to the size of unit cells of crystals or typical inorganic molecules – and characterised by an abundance of water. The numerical treatment of electrostatics thus needs to be both accurate and fast.

Electrostatic schemes can be roughly divided into *truncation methods* where all explicit interactions beyond a certain cutoff are ignored, and *long-range methods* which explicitly take all interactions into account. There is one important difference between the two classes: all *long-range* algorithms give, in principle, the same result and are thus interchangeable [7]. Their error is of numerical nature and can be tuned by, e.g., adjusting the number of terms included in series expansions [8,9,10,11]. Selecting one of them for a given application is primarily a technical decision. This is not the case for *truncation methods*, and the different truncation schemes are indeed different. Shifting functions and reaction field techniques are examples of methods that can be used instead of plain, abrupt truncation.

There have been many studies comparing different electrostatic schemes for systems such as water, ions, peptides, proteins, or lipids. To the best of our knowledge, the first of such articles was published more than 15 years ago [12]. Common to almost all of the earlier studies is the use of a very short cutoff

$r_{\text{cut}} \approx 1$ nm for truncation. Hence, the poor performance of truncation schemes in those studies is no surprise. Such short cutoffs are neither needed nor should be used with present-day computational resources, and there have been some recent studies on the differences between electrostatic schemes for cutoffs of at least 1.4 nm, namely for water [13,14,15], peptides [16], proteins [17,18,19], and lipids [20,21,22].

In this paper, we benchmark some of the most commonly used electrostatic schemes through extensive atomic-level MD simulations of lipid bilayer systems on some of the most common hardware, namely Pentium-4, IBM Power 4, and Apple/IBM G5. Additionally, we tested the parallel performance on Infiniband, GigaBit Ethernet, Fast Ethernet, and (N)UMA (nearly uniform memory architecture) networks. GROMACS software was used for the simulations since it is one of the most popular simulation engines in biophysical and soft matter simulations, and comes with open source code. There exists other well-established and widely used simulation packages, such as NAMD [23], Amber [24], and Charmm [25], to name some of the most common ones. While possibly being the least versatile of these, GROMACS is generally accepted as the fastest one on a single processor CPU due to its use of inner loops written in assembler. The increased speed within each node puts additional stress onto the network in a parallel simulation, thus allowing a good presentation of parallelisation limitations. It is expected that also in the future the speed of processor nodes will keep on increasing faster than the speed of the networks, and thus we believe that the results from Gromacs provide a fairly good representation of the behaviour on future computers. Although it would have been interesting, we did not have the resources to test other packages than GROMACS – the simulations presented here took approximately 22 000 CPU hours. General trends should be very similar and independent of the program package. We would like to point out, however, that parallel performance varies due to different implementations particularly in the case of the particle-mesh Ewald method (PME) as it depends on the evaluation of Fourier series – but again, the general trends are expected to be the same; many of the common simulation packages use the FFTW library [26] for Fast Fourier Transforms. Physical aspects, such as the appearance of various artifacts in physical observables, have been addressed in various other articles, e.g. Refs. [20,22], and will not be discussed here.

This paper is organised as follows. We first describe the modelling of the bilayer and the different electrostatic schemes employed here (Secs. 2 and 3). We then present the results of benchmarking (Sec. 4). The detailed presentation of the results is designed to allow the reader to compute how long a simulation of his/her own will take using a particular architecture – or whether such a simulation is feasible. Although we focus on benchmarking, a short discussion of the physical aspects is provided in Sec. 4. The discussion covers also more general aspects related to simulations of systems with Coulomb interactions.

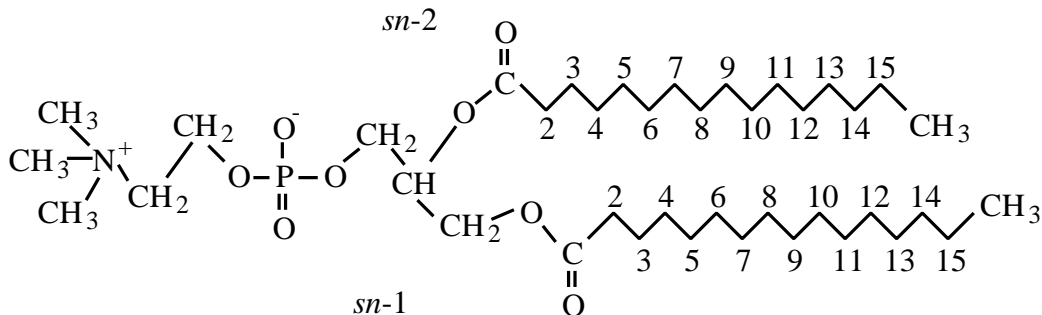


Fig. 1. DPPC molecule used in all bilayer simulations here.

2 Model and simulation details

As our benchmark system we used a single-component lipid bilayer comprised of 128 dipalmitoyl phosphatidylcholine (DPPC) molecules, see Fig. 1, fully hydrated by 3655 water molecules. To see the effect of increasing system size, membranes consisting of 512 and 2048 DPPC molecules were also simulated. DPPC molecules are described by the model from Ref. [27], available at <http://moose.bio.ucalgary.ca/Downloads/files/dppc.itp>, which utilises the description of lipids from Ref. [28], available at <http://moose.bio.ucalgary.ca/Downloads/files/lipid.itp>. The rigid SPC water model [29] was used for water. The simulations were started from a structure published in Ref. [27] (run E), available at <http://moose.bio.ucalgary.ca/Downloads/files/dppc128.pdb>.

The simulations were performed using the GROMACS simulation package [30]. The bond lengths of DPPC molecules were constrained by the LINCS algorithm [31] while SETTLE [32] was used for water. Those choices allowed a time step of 2.0 fs. For computing nonbonded interactions, we employed the twin-range setup [33], i.e., interactions within $r_{\text{list}} = 1.0$ nm were evaluated at every integration step, and interactions outside of r_{list} only every tenth integration time step.

Lennard–Jones interaction was cut off at 1.0 nm (with one exception, see Sec. 3.1.3). DPPC and water molecules were separately coupled to a heat bath at temperature $T = 323$ K, and the pressure was kept at 1 bar, both using the Berendsen algorithms [34]. The size of the simulation box in the plane of the bilayer (x - y plane) was allowed to fluctuate independently of its height. We present results of a few hundred short simulations with different system sizes and computer & network architectures. This was supplemented with several longer simulations, to compute essential quantities needed to characterise the bilayers, such as the area per lipid and, and to determine how these quantities depend on the chosen electrostatics scheme. Equilibrium was monitored the commonly used way by measuring the area per lipid. In total, the simulations

took about 22 000 hours of CPU time.

3 Schemes for electrostatic interactions

The electrostatic interaction between two point charges q_i and q_j depends only on their mutual separation r and is given by the well-known Coulomb law

$$V_{ij}(r) = \frac{q_i q_j}{4\pi\epsilon_0 r}, \quad (1)$$

and the total potential then follows from

$$V_{\text{total}} = \sum_{i < j} V_{ij}(r_{ij}). \quad (2)$$

As this interaction is long-ranged, the potential has to be replaced by some related potential $\mathcal{V}(r)$ that offers the advantage of being easier to compute.

3.1 Truncation methods

Truncation methods set $\mathcal{V}_{ij}(r) = 0$ for r larger than some cutoff r_{cut} . This reduces the computational cost from $\mathcal{O}(N^2)$ – all combinations of the N particles inside the simulation volume have to be considered – to $\mathcal{O}(Nr_{\text{cut}}^3)$. The saving is substantial if r_{cut} is much smaller than the extension of the simulation box. For the present study, we used $r_{\text{cut}} = 1.8$ nm, $r_{\text{cut}} = 2.0$ nm, and $r_{\text{cut}} = 2.5$ nm. Truncation can be done in different ways, the usual approaches being abrupt truncation, using shifting functions, or using the reaction field method.

3.1.1 Abrupt truncation

Conceptually the easiest approach is to set $\mathcal{V}_{ij}(r) = V_{ij}(r)$ for $r \leq r_{\text{cut}}$, and $\mathcal{V}_{ij}(r) = 0$ otherwise. This scheme leads to discontinuities in both electrostatic potential and force at the cutoff. The simulations done using this scheme are labelled by their value of r_{cut} throughout this paper.

3.1.2 Shifting functions

The abrupt truncation of the potential at r_{cut} can be avoided by modifying the potential $\mathcal{V}_{ij}(r)$ for $r_{\text{switch}} \leq r \leq r_{\text{cut}}$ such that both the resulting force and its derivative are continuous for all r . This is easily achieved by replacing

$\mathcal{V}_{ij}(r)$ in this interval by a third-order polynomial. Its coefficients are uniquely defined by the continuity requirements. Note that neither the potential nor the force are simply “shifted”. The name “switching function” thus captures the concept better than the commonly used name “shifting function”.

The choice for r_{switch} is, in principle, arbitrary. The two most common choices are $r_{\text{switch}} = 0$, or to set $r_{\text{switch}} = r_{\text{list}}$, i.e., the range of short-range interactions. We adopt the latter and thus set $r_{\text{switch}} = 1.0$ nm. We label the simulations employing a shifting function by their value of r_{cut} with the acronym SH.

3.1.3 Reaction field technique

The Onsager reaction field technique [35] handles all electrostatic interactions explicitly within the cutoff distance r_{cut} . For $r > r_{\text{cut}}$ the system is treated on a mean-field level and is thus completely described by its dielectric constant ϵ . The potential is

$$\mathcal{V}(r) = \frac{q_i q_j}{4\pi\epsilon_0 r} \left[1 + \frac{\epsilon - 1}{2\epsilon + 1} \left(\frac{r}{r_{\text{cut}}} \right)^3 \right] - \frac{q_i q_j}{4\pi\epsilon_0 r_{\text{cut}}} \frac{3\epsilon}{2\epsilon + 1} \quad \text{for } r \leq r_{\text{cut}} . \quad (3)$$

The second term makes the potential vanish at $r = r_{\text{cut}}$.

A reaction field description needs an additional input parameter, namely the dielectric constant ϵ . Its choice may be problematic in inhomogeneous systems such as hydrated lipid membranes, where $\epsilon \approx 80$ for water, $\epsilon \approx 25$ at the water-membrane interface and $\epsilon \approx 4$ inside the lipid bilayer [36]. We have used $\epsilon = 80$.

We mark reaction field results by the acronym RF. Since reaction field has been suggested to allow a smaller r_{cut} than other truncation schemes due to its mean-field accounting of the “cut-away” medium, we have included a simulation with a very short cutoff $r_{\text{cut}} = 1.2$ nm. In order to keep a twin-range setup, we also had to use a smaller $r_{\text{list}} = r_{\text{vdW}} = 0.9$ nm. (All other simulations were run using our standard choice $r_{\text{list}} = r_{\text{vdW}} = 1.0$ nm.)

3.2 Long-range methods

It is possible to have $\mathcal{V}_{ij}(r) \neq 0$ for an arbitrarily large r . Due to the finite size of the simulation box this implies that periodic boundary conditions are built as an integral part into the electrostatics evaluation scheme. Applying periodic boundary conditions and long-range electrostatics means that not only the direct interaction between two particles is considered but also the interaction between *all* of their mirror images. Considering the simulation

box as an entity, what one really wants is that *i*) all the particles in the mirror image of the simulation box have the same mutual correlations as in the original simulation box, and *ii*) all particles in the mirror image of the simulation box are uncorrelated with their "twin" in the original box. All long-range electrostatics schemes fulfil property *i*) exactly (in contrast to RF where this property is only fulfilled on a mean-field level) whereas they obviously totally fail property *ii*).

Long-range electrostatics are usually computed either by using fast multipole methods (FMM) [11], the (smooth) Particle-Mesh Ewald (PME) method, [37] or the particle-particle / particle-mesh method (P³M) [38,9]. Both P³M and PME are based on Ewald summation. In the Ewald summation the electrostatic potential can be written as [39]

$$U_{\text{Ewald}}(r) = \frac{1}{2} \sum_{i=1}^N \sum_{j=1}^N \sum_{|\mathbf{n}|=0}^{\infty} 'q_i q_j \frac{\text{erfc}(\alpha |\mathbf{r}_{ij} + \mathbf{n}|)}{|\mathbf{r}_{ij} + \mathbf{n}|} \quad (4)$$

$$+ \frac{1}{2\pi V} \sum_{i=1}^N \sum_{j=1}^N \sum_{\mathbf{k} \neq 0} q_i q_j \frac{4\pi^2}{k^2} \exp\left(-\frac{k^2}{4\alpha}\right) \times \cos(\mathbf{k} \cdot \mathbf{r}_{ij}) - \frac{\alpha}{\sqrt{\pi}} \sum_{i=1}^N q_i^2$$

Here q_i and q_j are the two charges, α is the Ewald parameter, \mathbf{k} is the reciprocal lattice vector, and $V = L_x \times L_y \times L_z$ is the volume of the system. The prime means that the term $i = j$ should be dropped for $\mathbf{n} = 0$ (the actual simulation box). Solving the above gives, at best, $\mathcal{O}(N^{3/2})$ scaling. PME and P³M are based on formulating the above equation in such a way that one can use the Fast Fourier Transform to obtain better scaling, $\mathcal{O}(N \ln N)$.

FMM offers the advantage of better scaling with system size [$\mathcal{O}(N)$ compared to $\mathcal{O}(N \ln N)$] of PME, but is more sensitive to numerical noise, more laborious to implement and is currently not included in major simulation packages. At the present time PME is the most frequently used algorithm, and we also use PME here. It should be stressed again that all methods for long-range electrostatics give the same result up to a numerical error (depending on grid spacing, number of k vectors, etc.) that can be made arbitrarily small in a controlled way at the expense of an increase in computational cost [9].

4 Results – speed and scalability

Simulations of biomolecular systems are typically limited by the lack of available computer power. Tables 1 and 2 list our benchmark results for different architectures and networks. We have studied lipid systems of various sizes on a varying number of nodes for parallel runs using all electrostatics schemes described in this paper. The three architectures – Pentium-4, IBM Power 4 and Apple/IBM G5 – represent the majority of computer systems used around

Pentium-4 2.4 Ghz (Fast Ethernet)												
nodes	8 × 8 lipids				16 × 16 lipids				32 × 32 lipids			
	1	2	4	8	1	2	4	8	1	2	4	8
1.8	17.4	10.1	8.9	7.1	77.9	47.4	33.3	30.4	322.1	186.1	123.1	89.2
2.0	20.4	12.6	9.2	7.2	89.3	52.2	35.7	30.7	368.3	222.2	131.4	96.4
2.5	27.9	16.4	11.4	8.2	130.3	71.9	43.9	36.5	543.6	307.5	172.1	118.5
SH 1.8	22.8	14.6	10.3	7.8	101.2	58.1	38.1	31.8	418.5	245.6	142.9	100.7
SH 2.0	25.8	16.2	11.0	8.1	114.7	63.5	41.1	34.9	475.7	266.4	158.5	106.1
SH 2.5	35.8	23.1	13.5	9.4	165.7	82.8	51.2	40.1	672.8	359.3	208.1	138.2
RF 1.2	11.5	8.5	7.4	6.2	49.7	36.2	26.7	26.7	201.0	141.1	95.3	77.4
RF 1.8	17.1	11.4	8.9	7.1	82.1	49.2	33.5	30.1	328.5	195.3	123.2	89.3
RF 2.0	20.0	13.5	9.6	7.4	91.9	53.9	35.8	31.7	380.1	221.4	135.0	96.5
RF 2.5	28.8	17.8	11.7	8.3	135.3	70.3	46.0	35.8	558.5	311.5	177.6	121.4
PME	27.4	39.4	63.6	82.2	116.9	154.9	244.9	323.9	480.0	624.7	964.4	1178.6

Pentium-4 2.66 Ghz (Gigabit Ethernet)												
nodes	8 × 8 lipids				16 × 16 lipids				32 × 32 lipids			
	1	2	4	8	1	2	4	8	1	2	4	8
1.8	15.3	7.4	5.3	3.6	73.1	37.9	21.8	15.7	295.0	147.2	81.4	52.2
2.0	17.8	10.3	6.5	3.6	81.9	41.7	24.2	15.8	334.0	178.8	91.4	54.6
2.5	25.3	12.6	7.8	4.9	118.1	54.2	31.0	21.7	497.2	244.2	129.9	76.4
SH 1.8	20.7	11.5	7.1	4.6	93.9	44.0	26.8	19.3	370.3	188.6	102.6	60.8
SH 2.0	23.5	12.2	7.4	4.6	109.2	53.9	29.2	19.7	431.2	212.1	115.8	65.8
SH 2.5	32.4	17.9	10.1	6.1	152.4	68.1	38.2	23.1	605.7	320.0	165.4	92.2
RF 1.2	10.3	5.8	3.8	2.8	46.1	25.8	14.6	10.4	184.6	93.9	60.1	33.2
RF 1.8	16.1	8.6	5.0	3.8	72.9	36.7	16.4	15.3	299.7	148.6	84.2	56.1
RF 2.0	18.5	10.8	6.1	4.2	84.0	39.9	23.9	18.3	347.4	181.9	89.4	56.4
RF 2.5	25.4	13.3	7.6	5.4	119.9	56.2	31.2	20.7	512.8	251.8	138.1	81.5
PME	25.0	20.3	17.6	20.8	108.8	82.8	81.4	79.7	428.9	329.6	283.8	243.9

Table 1

Hours of wall clock time needed per 1 ns of trajectory. The different columns correspond to different membrane sizes and different numbers of nodes (for parallel runs). The specified membrane size is the number of lipids per single leaflet. The studied bilayers thus contained twice that number of lipids.

the world. We did this with the intent of enabling the user to estimate the time that his/her own simulations will need. The user needs to pick one of our three test systems, closest to his/her own computational resources, and then simply scale our benchmark results with the difference in clock frequency.

First, we tested Pentium-4 CPUs running at 2.4 Ghz, connected by Fast Ethernet switches. We also used Pentium-4 CPUs running at 2.66 Ghz, connected by GigaBit Ethernet switches. Then, we used the Apple/IBM G5 based systems in which each node was a Dual 2.3 GHz PowerPC 970FX processor. The nodes were connected by Infiniband network. We also tested a network of Infiniband connected 3.4 GHz Pentium-4 CPUs. Finally, we used Power-4 nodes

Power-4 1.1 Ghz ((N)UMA nearly uniform memory access)												
nodes	8 × 8 lipids				16 × 16 lipids				32 × 32 lipids			
	1	2	4	8	1	2	4	8	1	2	4	8
1.8	27.9	13.8	7.2	3.9	118.5	55.6	30.0	17.2	471.8	232.9	130.0	71.0
2.0	32.1	15.8	8.8	5.0	131.1	63.6	37.8	20.8	572.1	269.4	167.4	84.6
2.5	44.9	21.8	12.2	5.7	191.4	87.9	50.0	25.7	759.2	323.9	205.8	100.6
SH 1.8	49.2	23.6	11.9	6.4	180.6	97.8	53.9	30.1	870.8	373.2	206.5	95.1
SH 2.0	55.6	27.2	14.9	6.5	212.4	109.0	58.2	34.6	916.7	421.5	239.9	141.2
SH 2.5	72.6	37.1	21.5	11.4	297.8	146.2	84.7	48.1	1246.7	600.4	419.3	197.5
RF 1.2	21.7	9.3	4.7	2.8	102.8	36.8	20.8	10.6	256.7	153.5	85.6	48.3
RF 1.8	31.5	15.1	7.8	4.4	109.7	62.2	34.9	17.1	504.4	245.6	142.2	85.3
RF 2.0	31.9	16.8	8.8	5.6	122.2	68.3	36.4	19.9	570.8	296.9	150.7	94.2
RF 2.5	48.2	23.6	13.5	6.2	197.4	93.6	56.8	25.6	819.9	437.8	221.1	67.1
PME	42.4	21.9	11.2	7.6	172.4	89.3	45.4	27.6	705.0	401.9	226.1	125.7

G5 2.3 GHz (Infiniband)												
nodes	8 × 8 lipids				16 × 16 lipids				32 × 32 lipids			
	1	2	4	8	1	2	4	8	1	2	4	8
1.8	11.0	5.4	3.1	1.9	52.8	22.8	11.9	7.1	237.8	100.7	52.6	28.8
2.0	12.8	6.1	3.6	2.2	60.6	25.6	13.6	8.2	271.9	115.8	61.2	32.8
2.5	17.9	8.6	4.6	3.1	95.3	35.6	19.0	10.7	380.7	161.2	92.8	47.8
SH 1.8	16.1	7.6	4.2	2.6	73.2	31.5	16.1	9.4	315.7	140.4	70.1	38.1
SH 2.0	18.1	8.9	4.7	2.6	84.9	35.6	18.6	10.6	360.3	153.8	80.3	42.8
SH 2.5	24.6	11.9	6.4	3.8	127.1	50.0	26.0	14.0	518.3	228.2	118.9	60.1
RF 1.2	8.2	3.9	2.4	1.7	36.2	16.4	8.6	5.3	156.4	69.2	37.2	20.6
RF 1.8	12.2	6.0	3.5	2.2	60.7	26.8	13.5	7.8	187.1	113.5	58.6	33.9
RF 2.0	14.2	6.7	3.8	2.4	69.4	29.7	15.6	9.0	311.7	128.6	65.4	37.8
RF 2.5	19.2	9.3	4.9	2.9	104.0	40.8	21.7	11.4	452.4	201.4	106.7	59.7
PME	18.5	9.9	6.1	4.9	81.7	40.8	24.7	17.8	334.6	179.3	106.2	67.8

Pentium-4 3.4 Ghz (Infiniband)												
nodes	8 × 8 lipids				16 × 16 lipids				32 × 32 lipids			
	1	2	4	8	1	2	4	8	1	2	4	8
1.8	17.4	8.2	4.3	2.4	76.1	33.1	16.8	8.9	309.4	135.8	68.6	35.6
2.0	19.4	9.3	4.9	2.6	85.7	36.8	18.8	10.1	349.4	152.4	77.6	40.1
2.5	27.1	12.9	6.5	3.5	121.1	51.4	26.4	13.8	339.0	215.6	110.4	56.5
SH 1.8	24.7	11.8	6.1	3.2	108.8	47.1	24.0	12.5	398.3	192.4	97.4	49.9
SH 2.0	27.9	13.3	6.8	3.6	122.2	53.2	26.8	14.0	334.3	218.1	109.9	56.5
SH 2.5	38.8	18.6	9.6	4.9	169.9	73.9	37.4	19.6	139.3	303.9	153.9	79.2
RF 1.2	11.5	5.6	3.1	1.8	50.0	22.1	11.4	6.1	205.4	90.3	46.4	23.9
RF 1.8	19.2	9.0	4.7	2.6	83.8	36.5	18.5	9.7	342.6	149.9	76.2	39.2
RF 2.0	21.5	10.4	5.3	2.8	94.7	41.1	21.1	11.1	388.8	169.9	86.5	44.7
RF 2.5	30.0	14.4	7.4	3.9	134.3	57.2	29.0	15.1	282.8	237.5	121.2	64.2
PME	21.8	11.0	6.1	3.9	96.4	45.0	24.4	14.7	386.2	182.2	99.3	58.2

Table 2

Hours of wall clock time needed per 1 ns of trajectory. The different columns correspond to different membrane sizes and different numbers of nodes (for parallel runs). The specified membrane size is the number of lipids per single leaflet. The studied bilayers thus contained twice that number of lipids.

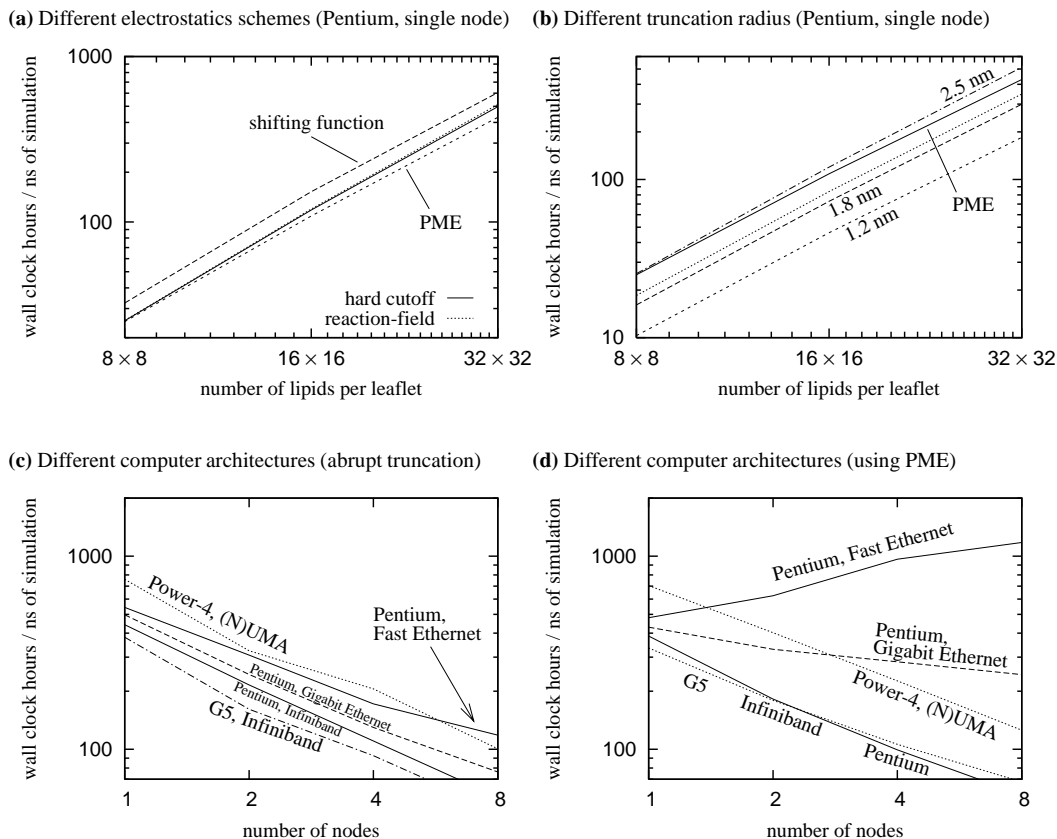


Fig. 2. (a) The time needed (hours of wall clock time) to compute a 1 ns trajectory for membranes of different size. The results are for a single Pentium-4 at 2.66 Ghz and $r_{\text{cut}} = 2.5$ nm. (b) Comparison of reaction field with different values of r_{cut} . (Remember that $r_{\text{cut}} = 1.2$ nm uses a smaller r_{list} .) (c) Benchmark results for truncation on the different architectures with a varying number of nodes used for parallel runs. N(UMA) stands for nearly uniform memory access. (d) Benchmark results for PME runs on the different architectures with a varying number of nodes used for parallel runs. Each leaflet contains 16×16 lipids.

running at 1.1 Ghz on an IBM eServer Cluster 1600 supercomputer. The latter has a nearly uniform memory architecture, i.e., communication between CPUs is possible by directly reading from or writing to other CPUs' local memory. For the eServer Cluster architecture, the speed difference is only a factor of 2.7 on the average (less than the speed difference between different levels of cache on a single Pentium-4 CPU) such that the name “almost-uniform memory architecture” captures the concept well.

4.1 Single processor performance

A selection of the single-processor results from Tables 1 and 2 (for $r_{\text{cut}} = 2.5$ nm) is shown graphically in Fig. 2a-b. Reaction field is slightly slower than abrupt truncation, while shifting function needs approximately 30 % more

time. In contrast to common belief, PME is faster than any of the truncation methods. We can only offer better cache utilisation as an explanation. We also found the relative positions of the curves to be almost independent of computer architecture. For $r_{\text{cut}} = 2.0$ nm, the relative performance of PME drops slightly and becomes equivalent to the use of shifting functions. Only for $r_{\text{cut}} = 1.8$ nm is PME slower than all the truncation methods we tested.

In order to understand these results we should recall that we have employed a twin-range setup in evaluating electrostatic interactions. Within a certain distance r_{list} , mutual electrostatic interactions (called short-range interactions) are evaluated at every integration step, while outside of r_{list} (called long-range part) this is done only every tenth integration step. For $r_{\text{cut}} = 1.8$ nm, for example, more than two thirds of the force evaluations are for short-range interactions. The scheme for treating the long-range part of electrostatic interactions thus has less influence than might be expected naively.

For the short-range part $r \leq r_{\text{list}}$, a potential with abrupt truncation is the easiest to compute since $r_{\text{cut}} > r_{\text{list}}$ and thus only the plain Coulomb’s law (without a cutoff) needs to be evaluated. The reaction field expression (3) is more complicated than Coulomb’s law (1). Since the additional terms such as r^2 need to be computed anyhow in order to compute $1/r$, the overhead is surprisingly small: the number of floating-point operations increases by less than 20 %. Since also the Lennard–Jones and bonded interactions and memory accesses take some time, the observed speed decrease is significantly lower than this.

The shifting scheme is particular in that the functional form of the potential changes at r_{switch} . A conditional statement is very expensive due to the high cost of flushing the CPU pipelines in case of a misprediction. For this reason, it is more efficient to implement shifting functions via a table containing $\mathcal{V}_{ij}(r)$ for discrete values of r . The lower speed of shifting functions compared to the other two truncation schemes reflects the higher computational cost of a table lookup and subsequent interpolation compared to direct evaluation of a straight-forward potential.

During the short-range electrostatics evaluation in the switching scheme, $\mathcal{V}(r)$ is computed for values of r that can be slightly larger than r_{list} . This is because the test $r < r_{\text{list}}$ is applied to the entire charge group, and the test is done only during a neighbour-list rebuild. Still, it should be noted that for $r_{\text{list}} \gg r_{\text{switch}}$ the short-range electrostatics evaluation can use the computationally cheaper direct evaluation of the Coulomb potential (1). Unfortunately, specialised treatment for this case is not implemented into GROMACS, and it would also not be beneficial for us as we use $r_{\text{switch}} = r_{\text{list}}$.

When PME is employed, the short-range part of the potential is given by

the complementary error function. Since this function is very expensive to compute, a tabulated potential is used. In view of the speed of tabulated shifting functions, the very competitive speed of PME demonstrates that it is a very efficient method for computing the long-range part of the potential – its speed is able to compensate for the slowness of the short-range evaluation.

As discussed above, more time is spent on computing the short-range part of the potential than on the long-range part. The total number of electrostatic evaluations thus only increases by a factor 1.6 in going from $r_{\text{cut}} = 1.8$ nm to $r_{\text{cut}} = 2.5$ nm instead of the naively expected factor $(2.5/1.8)^3 \approx 2.7$. An example for the time increase with increasing r_{cut} is shown in Fig. 2b for reaction field. (Remember that for $r_{\text{cut}} = 1.2$ nm we employ $r_{\text{list}} = 0.9$ nm instead of the standard value $r_{\text{list}} = 1.0$ nm. Most of the speed increase seen in the figure for $r_{\text{cut}} = 1.2$ nm stems from this.)

4.2 Scalability

Apart from the intrinsic speed of an electrostatics scheme, its parallelisability is of great importance. Over the past years, the size of the biosystems that are studied has increased faster than the speed of a single CPU, thereby increasing the need for parallel simulations. Figure 2a-c show a few selected benchmark results for PME and abrupt truncation. The scaling results for all truncation schemes are basically identical, and scaling is influenced surprisingly little by the size of the lipid membrane. A closer analysis of Tables 1 and 2 shows that on the IBM eServer supercomputer, especially for reaction field, quite a few instances of superlinear scaling are observed. The appearance of superlinear scaling itself can be explained by an increase of the total available cache space with increasing number of nodes but we cannot offer an explanation why this is more prominent for reaction field than for the other truncation methods. Figure 2d shows that truncation methods scale very well on all the architectures we studied. On a supercomputer, PME scales as well as the truncation methods. However when PME was used on Gigabit Ethernet, the wall clock time needed decreased only slightly when the number of nodes is increased, and with Fast Ethernet the time actually increased with number of nodes. These results for different network architectures let us to conclude that using GROMACS (at least), it is thus senseless to use parallel PME if only Fast Ethernet is available and it is doubtful even when using Gigabit Ethernet.

This can partly explain why relatively little attention has been given to benchmarking parallel electrostatics until recently. In the days when most numerical work was done at a few supercomputing centres, every electrostatics scheme would perform approximately equally well. Only with the advent of cheap Linux clusters, the problem of poor scaling of, e.g., PME arose.

The numerical work for computing the long-range part of the potential is mainly given by the work needed for the FFT. As all commonly used programs employ the same FFTW library, they have in principle the same limitations for scalability. Programs differ, however, as well as different methods like PME vs. P3M differ, in their distribution of work between the Fourier part and the direct summation. The distribution employed by GROMACS, which by default does not depend on the number of nodes, is somewhat suboptimal in this aspect. Other programs might improve scalability by shifting more work to the direct summation while increasing the FFT grid spacing, thereby reducing the work done by the FFT that is parallelising worse than the direct summation.

5 Discussion

In this paper, we have used a lipid membrane as test bed to examine various schemes commonly used to handle electrostatics in atomistic MD simulations of biomolecular systems. We compared different truncation schemes (abrupt truncation, shifting function and reaction field) and the particle-mesh Ewald technique. The focus here was on speed and performance on different architectures and networks. All of these schemes have been treated on an equal footing, i.e., all interactions have been identical except for the scheme used for computing the electrostatic interactions.

On the hardware side, the Apple/IBM G5 based system performed very well showing the strengths of the architecture. Earlier this year, Apple started moving from the IBM G4/G5 chips to Intel processors which seems to mark the end of an era. Similarly, another good performer, the DEC Alpha processor, was phased out a few years back.

On the physical side, an abrupt truncation of electrostatic interactions should be avoided [20,21,22]. It introduces major artifacts into the system without offering any noteworthy benefits in speed compared to, e.g., reaction field techniques. Shifting functions, reaction field technique and PME all offer results of good quality even though the quantitative results disagree somewhat. This can be fixed, e.g., by tuning the force field but care should be taken: recent studies have shown that even the RF method should be used with great care in cases of bulk water [40]. Of more interest is thus the following question: given a force field developed for some particular electrostatics scheme, which other schemes can be substituted without the need to reparameterise the force field?

We also found (data not shown) that the results for the shifting function and reaction field are only moderately dependent on r_{cut} . (The only exception to

this statement is $r_{\text{cut}} = 1.2$ nm. In our opinion, $r_{\text{cut}} = 1.2$ nm should be avoided in membrane simulations altogether.) This dependence seems to be even a bit smaller for the reaction field than for the shifting function. This, however, depends on the weight assigned to the different quantities studied in this paper. This weak dependence on r_{cut} allows for choosing a small value of r_{cut} . On the other hand, our benchmarks demonstrate that the cost of using a larger cutoff is smaller than might be naively expected.

From studying a large number of different quantities that could not be displayed here for space restrictions, we found that RF and PME are interchangeable, i.e., going from one scheme to the other changes the results only by a margin that is comparable with experimental uncertainty. This property is the main advantage of reaction field over shifting functions. There is, however, one important question: given a force field developed for some particular electrostatics scheme, with a particular value of the r_c for a truncation method, is it possible to change that value or even to choose a completely different scheme – without the need to reparameterise the force field? Here, we have not tried to answer that question, but it should be kept in mind whenever different methods with various force fields are being chosen and tested.

Our testbench in this study was the GROMACS simulation engine. As mentioned in the beginning, GROMACS is by no means the only possible simulation engine. However, we expect the trends be largely similar independent of the software package. In the case of Ewald summation based electrostatics, performance depends heavily on the Fast Fourier Transform library. The FFTW library [26] is a common choice, and packages such as GROMACS, Amber [24], NAMD [41,23], LAMMPS [42], and Espresso [43] use FFTW. Some of the packages also offer other options for performing FFTs, but the FFTW library is by far the most popular in the field.

There are also other methods for evaluating electrostatic interactions, but these are not as widely used as PME. The P³M method is another efficient Ewald-based scheme. Other developments on the Ewald-based methods have appeared recently [44,45]. Of the methods that are not based on Ewald summation, the Fast Multipole Method, [11,46,47] often called just FMM, is a different set of methods utilising the multipole expansion. It offers better scaling, as it is an $\mathcal{O}(N)$ algorithm. This, however, comes with the expense of larger prefactors. Multigrid methods [48,49] are also newcomers, offering, like FMM, $\mathcal{O}(N)$ scaling. These methods also natively include other boundary conditions than the usual periodic ones. Another novel $\mathcal{O}(N)$ algorithm is the method of Maggs *et al.* [50,51] which is based on propagating the electric field and solving the Maxwell’s equations. However, we did not test the above non-Ewald algorithms as standardised (à la GROMACS or NAMD) implementations do not (to our knowledge) exist.

Finally, it is worth noticing that Ewald summation -based methods are typically fast and suitable only in fully periodic systems. If periodicity is broken, e.g., by the presence of a wall, the method needs to be modified. This strongly affects the performance. Alternatively, other methods need to be used. For Ewald-based methods there are several possible variants. These typically use the trick of adding an extra dipolar term, and including empty space in the simulation box [52]. A review and comparison of many of the earlier Ewald-based methods for slab geometries has been written by Widmann and Adolf [53]. There have been many new developments to include boundary conditions other than periodic. Of the above methods, FMM, multigrid, and the methods of Maggs *et al.* natively include other boundary conditions. Other methods include Lekner summation [54] and the MMM2D method [55].

In summary, long-range interactions, such as the Coulomb interaction, still pose challenges to simulators. This is clearly demonstrated by the large number of articles published on these topics over the last few years. Modellers need to take care in choosing an appropriate method, one that maximises computational efficiency, at the same time giving reliable results.

Acknowledgements

This work has been supported by the Academy of Finland Centre of Excellence Program, the Academy of Finland, the Jenny and Antti Wihuri Foundation, the Federation of Finnish Insurance Companies, the Emil Aaltonen Foundation, the European Union Marie Curie fellowship HPMF-CT-2002-01794 (M.P.), European Program MRTN-CT-2004-512331 (M.P.), and by the Beckman Institute Fellows program (E.F.). We would also like to thank the Finnish IT Centre for Science (CSC), the supercluster computing facility at the University of Southern Denmark, Center for Parallel Computers at the Royal Institute of Technology in Stockholm, the Terascale Computing Facility at Virginia Polytechnic Institute & State University for computational resources, and the Laboratory for Computational Engineering at the Helsinki University of Technology.

References

- [1] T. Schlick, *Molecular Modeling and Simulation*, Vol. 21 of *Interdisciplinary Applied Mathematics*, Springer Verlag, New York, NY, 2002.
- [2] H. L. Scott, Modeling the lipid component of membranes, *Curr. Opin. Struct. Biol.* 12 (2002) 495–502.

- [3] T. Schlick, R. D. Skeel, A. T. Brunger, L. V. Kalé, J. A. Board Jr., J. Hermans, K. Schulten, Algorithmic challenges in computational molecular biophysics, *J. Comput. Phys.* 151 (1) (1999) 9–48.
- [4] K. M. Merz, Jr., B. Roux (Eds.), *Biological membranes: A molecular perspective from computation and experiment*, Birkhäuser, Boston, 1996.
- [5] L. Saiz, M. L. Klein, Computer simulation studies of model biological membranes, *Acc. Chem. Res.* 35 (6) (2002) 482–489.
- [6] S. W. Chiu, E. Jacobsson, R. J. Mashl, H. L. Scott, Cholesterol-induced modifications in lipid bilayers: A simulation study, *Biophys. J.* 83 (2002) 1842–1853.
- [7] C. Sagui, T. Darden, Molecular dynamics simulations of biomolecules: Long-range electrostatic effects, *Ann. Rev. Biophys. Biomol. Struct.* 28 (1999) 155.
- [8] J. Kolafa, J. W. Perram, Cutoff errors in the Ewald summation formulae for point charge systems, *Mol. Sim.* 9 (5) (1992) 351–368.
- [9] M. Deserno, C. Holm, How to mesh up Ewald sums. I. A theoretical and numerical comparison of various particle mesh routines, *J. Chem. Phys.* 109 (18) (1998) 7678–7893.
- [10] M. Deserno, C. Holm, How to mesh up Ewald sums. II. An accurate error estimate for the particle-particle-particle-mesh routines, *J. Chem. Phys.* 109 (18) (1998) 7694.
- [11] L. Greengard, V. Rokhlin, A fast algorithm for particle simulation, *J. Comput. Phys.* 135 (1997) 280–292.
- [12] H. E. Alper, R. M. Levy, Computer simulations of the dielectric properties of water: Studies of the simple point charge and transferrable intermolecular potential models, *J. Chem. Phys.* 91 (1989) 1242–1251.
- [13] B. Hess, Determining the shear viscosity of model liquids from molecular dynamics simulations, *J. Chem. Phys.* 116 (2002) 209–217.
- [14] H. Alper, R. M. Levy, Dielectric and thermodynamic response of a generalized reaction field model for liquid state simulations, *J. Chem. Phys.* 99 (12) (1993) 9847–9852.
- [15] H. E. Alper, D. Bassolino, T. R. Stouch, Computer simulation of a phospholipid monolayer-water system: The influence of long range forces on water structure and dynamics, *J. Chem. Phys.* 98 (1993) 9798–9807.
- [16] H. Schreiber, O. Steinhauser, Cutoff size does strongly influence molecular dynamics results on solvated polypeptides, *Biochemistry* 31 (25) (1992) 5856–5860.
- [17] J. D. Faraldo-Gómez, G. R. Smith, M. S. Sansom, Setting up and optimization of membrane protein simulations, *Eur. Biophys. J.* 31 (2002) 217–227.

- [18] D. P. Tieleman, B. Hess, M. S. P. Sansom, Analysis and evaluation of channel models: Simulations of alamethicin, *Biophys. J.* 83 (2002) 2393–2407.
- [19] D. M. York, T. A. Darden, L. G. Pedersen, The effect of long-range electrostatic interactions in simulations of macromolecular crystals: A comparison of the Ewald and truncated list methods, *J. Chem. Phys.* 99 (1993) 8345–8348.
- [20] M. Patra, M. Karttunen, M. T. Hyvönen, P. Lindqvist, E. Falck, I. Vattulainen, Molecular dynamics simulations of lipid bilayers: Major artifacts due to truncating electrostatic interaction, *Biophys. J.* 84 (2003) 3636–3645.
- [21] C. Anézo, A. H. de Vries, H.-D. Höltje, D. P. Tieleman, S.-J. Marrink, Methodological issues in lipid bilayer simulations, *J. Phys. Chem. B* 107 (2003) 9424–9433.
- [22] M. Patra, M. Karttunen, M. T. Hyvönen, E. Falck, I. Vattulainen, Lipid bilayers driven to a wrong lane in molecular dynamics simulations by truncation of long-range electrostatic interactions, *J. Phys. Chem. B* 108 (2004) 4485–4494.
- [23] J. C. Phillips, R. Braun, W. Wang, J. Gumbart, E. Tajkhorshid, E. Villa, C. Chipot, R. D. Skeel, L. Kale, K. Schulten, Scalable molecular dynamics with NAMD, *J. Comput. Chem.* 26 (2005) 1781–1802.
- [24] D. A. Case, T. E. Cheatham, III, T. Darden, H. Gohlke, R. Luo, K. M. Merz, Jr., A. Onufriev, C. Simmerling, B. Wang, R. Woods, The Amber biomolecular simulation programs, *J. Comput. Chem.* 26 (2005) 1668–1688.
- [25] B. R. Brooks, R. E. Bruccoleri, B. D. Olafson, D. J. States, S. Swaminathan, M. Karplus, CHARMM: A program for macromolecular energy, minimization, and dynamics calculations, *J. Comput. Chem.* 4 (1983) 187–217.
- [26] M. Frigo, S. G. Johnson, The design and implementation of FFTW3, *Proc. IEEE* 93 (2005) 216–231.
- [27] D. P. Tieleman, H. J. C. Berendsen, Molecular dynamics simulations of a fully hydrated dipalmitoylphosphatidylcholine bilayer with different macroscopic boundary conditions and parameters, *J. Chem. Phys.* 105 (1996) 4871–4880.
- [28] O. Berger, O. Edholm, F. Jahnig, Molecular dynamics simulations of a fluid bilayer of dipalmitoylphosphatidylcholine at full hydration, constant pressure, and constant temperature, *Biophys. J.* 72 (1997) 2002–2013.
- [29] H. J. C. Berendsen, J. P. M. Postma, W. F. van Gunsteren, J. Hermans, Interaction models for water in relation to protein hydration, in: B. Pullman (Ed.), *Intermolecular Forces*, Reidel, Dordrecht, 1981, pp. 331–342.
- [30] E. Lindahl, B. Hess, D. van der Spoel, GROMACS 3.0: a package for molecular simulation and trajectory analysis, *J. Mol. Model.* 7 (2001) 306–317.
- [31] B. Hess, H. Bekker, H. J. C. Berendsen, J. G. E. M. Fraaije, LINCS: A linear constraint solver for molecular simulations, *J. Comp. Chem.* 18 (1997) 1463–1472.

- [32] S. Miyamoto, P. A. Kollman, SETTLE: an analytical version of the SHAKE and RATTLE algorithms for rigid water models, *J. Comput. Chem.* 13 (1992) 952–962.
- [33] T. C. Bishop, R. D. Skeel, K. Schulten, Difficulties with multiple time stepping and fast multipole algorithm in molecular dynamics, *J. Comput. Chem.* 18 (1997) 1785–1791.
- [34] H. J. C. Berendsen, J. P. M. Postma, W. F. van Gunsteren, A. DiNola, J. R. Haak, Molecular dynamics with coupling to an external bath, *J. Chem. Phys.* 81 (1984) 3684–3690.
- [35] L. Onsager, Electric moments of molecules in liquids, *J. Am. Chem. Soc.* 58 (1936) 1486–1493.
- [36] R. B. M. Koehorst, R. B. Spruijt, F. J. Vergeldt, M. A. Hemminga, Lipid bilayer topology of the transmembrane-helix of M13 major coat protein and bilayer polarity profile by site-directed fluorescence spectroscopy, *Biophys. J.* 87 (2004) 1445–1455.
- [37] U. Essman, L. Perela, M. L. Berkowitz, H. L. T. Darden, L. G. Pedersen, A smooth particle mesh Ewald method, *J. Chem. Phys.* 103 (1995) 8577–8592.
- [38] R. W. Hockney, J. W. Eastwood, *Computer simulation of particles*, IOP Publishing Ltd, 1988.
- [39] M. P. Allen, D. J. Tildesley, *Computer Simulation of Liquids*, Clarendon Press, Oxford, 1987.
- [40] Y. Yonetani, Liquid water simulation: A critical examination of cutoff length, *J. Chem. Phys.* 124 (2006) 204501.
- [41] L. Kalé, R. Skeel, M. Bhandarkar, R. Brunner, A. Gursoy, N. Krawetz, J. Phillips, A. Shinozaki, K. Varadarajan, K. Schulten, NAMD2: Greater scalability for parallel molecular dynamics, *J. Comput. Physics* 151 (1999) 283–312.
- [42] S. J. Plimpton, Fast parallel algorithms for short-range molecular dynamics, *J. Comput. Phys.* 117 (1995) 1–19.
- [43] H. J. Limbach, A. Arnold, B. A. Mann, C. Holm, ESPResSo—an extensible simulation package for research on soft matter systems, *Comp. Phys. Comm.* 174 (2006) 704–727.
- [44] K. Nam, J. Gao, D. M. York, An efficient linear-scaling Ewald method for long-range electrostatic interactions in combined QM/MM calculations, *J. Chem. Theory and Comput.* 1 (2005) 2–13.
- [45] Y. Shan, J. L. Klepeis, M. P. Eastwood, R. O. Dror, D. E. Shaw, Gaussian split Ewald: A fast Ewald mesh method for molecular simulation, *J. Chem. Phys.* 122 (2005) 054101.

- [46] T. Hrycak, V. Rokhlin, An improved fast multipole algorithm for potential fields, *SIAM J. Sci. Comp.* 19 (1998) 1804–1826.
- [47] L. Ying, G. Biros, D. Zorin, A kernel-independent adaptive fast multipole algorithm in two and three dimensions, *J. Comput. Phys.* 196 (2004) 591–626.
- [48] C. Sagui, T. Darden, Multigrid methods for classical molecular dynamics simulations of biomolecules, *J. Chem. Phys.* 114 (15) (2001) 6578–6591.
- [49] J. A. Izaguirre, S. S. Hampton, T. Matthey, Parallel multigrid summation for the N-body problem, *J. Parall. Distrib. Comp.* 65 (2005) 949–962.
- [50] A. C. Maggs, V. Rossetto, Local simulation algorithms for Coulomb interactions, *Phys. Rev. Lett.* 88 (2002) 196402.
- [51] J. Röttler, A. C. Maggs, Local molecular dynamics with coulombic interactions, *Phys. Rev. Lett.* 93 (2004) 170201.
- [52] I.-C. Yeh, M. L. Berkowitz, Ewald summation for systems with slab geometry, *J. Chem. Phys.* 111 (7) (1999) 3155–3162.
- [53] A. H. Widmann, D. B. Adolf, A comparison of Ewald summation techniques for planar surfaces, *Computer Physics Comm.* 107 (1997) 167–186.
- [54] J. Lekner, Summation of Coulomb fields in computer-simulated disordered systems, *Physica A* 176 (1991) 485–498.
- [55] A. Arnold, C. Holm, MMM2D: A fast and accurate summation method for electrostatic interactions in 2d slab geometries, *Computer Physics Comm.* 148 (2002) 327–348.